Azithromycin Plus Zinc Sulfate Rapidly and Synergistically Suppresses IκBα-Mediated In Vitro Human Airway Cell ACE2 Expression for SARS-CoV-2 Entry

Chia-Wei Chang[1]†, Ming-Cheng Lee[2]†, Bor-Ru Lin[2,3], Yen-Pei Lu[1], Yih-Jen Hsu[2], Chun-Yu Chuang[4], Tsung-Tao Huang[1]*, Yin-Kai Chen[5,6]*

[1]Biomedical Platform and Incubation Service Division, Taiwan Instrument Research Institute, National Applied Research Laboratories, Hsinchu, Taiwan.

[2]Department of Internal Medicine, National Taiwan University Hospital, Taipei, Taiwan.

[3]Department of Integrated Diagnostics and Therapeutics, National Taiwan University Hospital, Taipei, Taiwan.

[4]Department of Biomedical Engineering and Environmental Sciences, National Tsing Hua University, Hsinchu, Taiwan.

[5]Graduate Institute of Clinical Medicine, College of Medicine, National Taiwan University, Taipei, Taiwan.

[6]Department of Hematology, National Taiwan University Cancer Center, Taipei, Taiwan.

†Equally contributed to this work.

***Correspondence to**：

Tsung-Tao Huang, Ph. D.

Biomedical Platform and Incubation Services Division

Taiwan Instrument Research Institute, National Applied Research Laboratories, Hsinchu, Taiwan

3F, 8, Sec. 2, Sheng Yi Rd., Zhubei City, Hsinchu County, 30261, Taiwan

E-mail：tthuang@narlabs.org.tw

Phone: +886-3-6676822 ext 3063

FAX: +886-3-6585676

Yin-Kai, Chen, MD

Department of Hematology, National Taiwan University Cancer Center, Taipei, Taiwan.

No.57, Ln. 155, Sec. 3, Keelung Rd., Da'an Dist., Taipei 106, Taiwan

Email：b8201032@tmu.edu.tw

Phone：+886223220322 ext 53996

Abstract

Large-scale efforts have been persistently undertaken for medical prophylaxis and treatment of COVID-19 disasters worldwide. A variety of novel viral spike protein-targeted vaccine preparations have recently been clinically distributed based on accelerated approval. We revisited the early but inconclusive clinical interest in the combination of azithromycin and zinc sulfate repurposing with safety advantages. In vitro proof of concept was provided for rapid and synergistic suppression of ACE2 expression following treatments in human airway cells, Calu-3 and H322M. The two representative ACE2-expressing human airway cells indicate the upper and lower respiratory tracts. Prophylactic and early therapeutic roles of azithromycin combined with zinc are proposed for virus cellular entry prevention potential bridging to effective antibody production.

Running Title

Azithromycin Plus Zinc Sulfate Suppresses Airway ACE2

Introduction

Cell surface ACE2 of the respiratory tract is a well-established critical entry of SARS-CoV-2 into infected cells (12, 42, 45). ACE2 mRNA expression was shown to be reduced from tracheobronchial to bronchioloalvelar regions. ACE2 expression was upregulated following viral infections (21, 37), interferon exposure (14, 37) and smokers (21, 37). It was postulated that hyperactivation of the transcription factor NF-κB following ACE2-mediated viral entry, most likely in nonimmune cells, including lung epithelial cells, resulted in cytokine release syndrome (11). NF-κB is a major transcription factor that regulates the genes responsible for both the innate and adaptive immune responses. Human type II pneumocytes (AT2) are one of the primary targets for SARS-CoV-2 infection (14). It was shown in an induced pluripotent stem cell-derived AT2 model that NF-κB signaling was rapidly and persistently upregulated upon SARS-CoV-2 infection (15).

Azithromycin (AZT), a second-generation macrolide with broad spectrum antibacterial activity, has drawn very early clinical attention in hot drug repurposing for the recurrence of COVID-19 patients. (3, 8, 20, 32) In addition to its antimicrobial activity resulting from inhibition of bacterial protein synthesis (39), AZT has been shown to protect against viral entry into A549 lung cancer cell lines (40) as well as viral infections of airway epithelial cells through reduced viral replication and increased interferon responses (9, 26, 34). AZT was demonstrated in vivo to suppress NF-κB activation and concomitant pulmonary inflammation (38). TNF-α-induced NF-κB DNA binding activity, IκBα degradation and IL-6/IL-8 release in tracheal cells of human origin were shown to be inhibited in vitro following AZT treatments in a

dose-dependent manner (1).

Zinc is a trace element supplement with clinical benefits in a variety of respiratory tract infections (43). In the United States, one of the major countries with the SARS-CoV-2 pandemic, there was an increased risk of zinc deficiency between 1992 and 2011 (19). Patients with COVID-19 disease had significantly lower serum zinc levels than normal controls (17). More complications developed in COVID-19 patients with zinc deficiency (17). The prophylactic and therapeutic roles of zinc supplementation are currently under investigation. (18, 33) Prevention of viral entry has been postulated to be one potential mechanism of zinc antiviral actions (43). Increased NF-κB DNA binding activity and IκBα mRNA expression were reported in lungs from a sepsis model of mice under zinc deficiency (2).

Short-course AZT has long been used clinically for atypical pneumonias with excellent safety and tolerability. Zinc supplementation is a relatively popular companion with vitamin complexes. Here, we showed markedly synergistic ACE2 suppression in two distinct ACE2-expressing human airway cells by combination treatments of AZT and zinc. Accordingly, we provided laboratory support to repurpose AZT plus zinc for early clinical intervention of COVID-19 disease.

Results and discussion

Because the lung is the primary and lethal organ of COVID-19 disease, Calu-3, H322M, H522, H460, H1299 and A549 human airway cells were screened for endogenous ACE2 expression. Calu-3, widely used for COVID-19 studies, and H322M were selected for subsequent exploration because of their endogenous ACE2 expression (Fig. 1A). The Calu-3 cells generated from human proximal bronchial adenocarcinoma (36) is characterized by features of differentiated, functional human airway epithelial cells (6). Calu-3 was also proposed to be a suitable model of the human nasal mucosa (16). Bronchoalveolar lavage analyses from COVID-19 patients

disclosed aberrant macrophage and T cell responses (22) as well as bronchoalveolar immune hyperactivation (44). Our drug repurposing for the critical bronchoalveolar involvement of COVID-19 disease was investigated with H322M, a bronchioalveolar cell line, in addition to Calu-3 for proximal airway involvement.

Rapid improvements in symptoms, including fever, dyspnea and hypoxia, were reported in a consecutive case series receiving high-dose zinc rescue with different preparations. (5) A randomized controlled trial for high-dose intravenous zinc was initiated as adjunctive therapy in SARS-CoV-2-positive critically ill patients (30). H322M was therefore treated with 24-hour serial doses of 18.75, 37.5, 75, 150 and 300 μM ZnSO4 (Zn) (Fig. 1B). Zn at 300 μM was determined for the subsequent drug repurposing combination study because ACE2 expression was potentially decreased following 24 hours of treatment (Fig. 1B). AZT at 50 μM was required to produce significant in vitro anti-rhinoviral activities of human bronchial epithelial cells from donors (9) and children with cystic fibrosis (34). Lower in vitro anti-rhinoviral levels of AZT were also reported for bronchial epithelial cells from COPD patients (26). Accordingly, H322M was treated with 24-hour serial doses of 50, 25, 12.5, 6.25 and 3.125 μM (Fig. 1C). An AZT concentration of 50 μM was chosen for the Zn combination because ACE2 expression was significantly decreased following 24 hours of treatment (Fig. 1C).

The most impressive finding of the present study was rapidly suppressed endogenous ACE2 expression of H322M under 24-hour treatments of 300 μM Zn combined with 50 and 25 μM AZT (Fig. 2A and 3A). Compared to 50 and 25 μM AZT treatments alone, 300 μM Zn showed a significantly synergistic suppressive effect on ACE2 expression (Fig. 2A and 3A). ACE2 expression was further decreased following 48-hour treatments with Zn and AZT combinations, especially 50 μM AZT (Fig. 2B). ACE2 mRNA expression of Calu-3 was significantly reduced following 24-hour

treatments of 300 μM Zn alone and in combination with 50 and 25 μM AZT (Fig. 3C). The markedly suppressive effect on ACE2 protein expression of Calu-3 was found 24 hours later following suppression of its ACE2 expression. Similar to H322M, 48-hour combination treatment with 300 μM and 50 μM AZT showed the most suppressive effect on ACE2 expression (Fig. 2D).

Certain NF-κB dimeric transcription factors and their activities are tightly repressed by 3 inhibitors, IκBα, IκBβ and IκB□, through the formation of stable IκB–NF-κB complexes. It was demonstrated that rapid degradation of free IκBα is critical for NF-κB activation (24). Our H322M associated results indicated that combination treatments of Zn and AZT altered IκBα degradation and contributed to rapid repression of endogenous ACE2 (Fig. 2A, 2B, 3A and 3B). Such synergistic effects were most prominent following 24-hour treatment with 300 μM Zn and 50 μM AZT (Fig. 2A and 2B). In contrast to the synergistic effect on IκBα degradation in H322M, IκBα expression was rapidly upregulated following 24-hour treatments with 300 μM combined with 50 and 25 μM AZT (Fig. 2C and 3D). A similar synergistic ACE2 suppressive effect was most prominent following 48 hours of 300 μM Zn treatment combined with 50 μM AZT (Fig. 2C and 2D). Accordingly, the underlying mechanisms of IκBα involved in ACE2 repression might be cell type specific and worth further investigation.

Membrane-tethered MUC1 belongs to one of the major components of mucus (29). In vitro MUC1 overexpression was demonstrated to limit influenza A virus (IAV) infection (25). It was shown in vivo that MUC1 expression not only impeded IAV but also reduced IAV disease severity (25). NF-κB activation in vitro via Toll-like receptor (TLR) pathways, including TLR 2, 3, 4, 5, 7 and 9, was counteracted by MUC1 overexpression (41). There is increasing evidence and therapeutic interest in TLR pathway modulations for COVID-19 disease (27, 28, 31). Elevated MUC1

mucin protein levels were found in the airway mucus of critically ill COVID-19 patients (23). Another interesting finding of the present study was that MUC1 expression in H322M and Calu-3 cells was most significantly increased following 24 hours of treatment with 300 μM Zn alone and to a lesser degree after treatment with 50 and 25 μM AZT (Fig. 4A and 4B).

The largest published retrospective case series reported that early outpatient treatment with zinc plus low-dose hydroxychloroquine and azithromycin significantly reduced the hospitalization rate (4). Compared with the hydroxychloroquine-based standard of care, the addition of AZT did not show improved clinical outcomes in an open-label multicenter randomized clinical trial performed among patients with severe respiratory COVID-19 disease in Brazil (7). On the other hand, large-scale randomized trials did not reveal the clinical benefits of hydroxychloroquine in patients with COVID-19 (10, 35). Accordingly, the feasible clinical timing and choice of combinations with AZT remain to be determined.

A computed model of the AZT-Zn^{++} complex demonstrated its potential against the replication and assembly of SARS-CoV-2 particles. We are the first to present in vitro evidence that Zn combined with AZT rapidly and significantly suppresses endogenous ACE2 expression and increases MUC1 expression in Calu-3 and H322M cells, representative of the human upper and lower respiratory tracts, respectively. Both ACE2 suppression and increased MUC1 expression were consistently demonstrated in the two human airway cells, indicating the prophylactic as well as early therapeutic potential of the AZT and Zn repurposing combination for COVID-19 disease. With threats of mutations located on the viral spike protein (13), we demonstrated a potentially rapid bridging way to effective antibody production by suppressing the key of virus cellular entry with fewer concerns of increasing viral mutations as well as safety and storage of novel vaccine preparations. The effective high-dose combination

of Zn and AZT shown here could be translated into a loading dosing modality in preclinical studies and clinical trials.

Materials and Methods

Cell lines and drug treatments

The H322M, H522, H460 and A549 human airway cells were courtesy of SLY (National Taiwan University), and the H1299 lung cancer cell line was courtesy of CCH (National Taiwan University Hospital). Calu-3 human upper airway cells were purchased from the American Type Culture Collection (ATCC) (Manassas, VA, USA). The Calu-3 cells were cultured with MEM (Thermo Fisher Scientific, Waltham, MA, USA) containing 20% (v/v) fetal bovine serum (Thermo Fisher Scientific), 100 mM sodium pyruvate, nonessential amino acids and penicillin-streptomycin in a humidified 5% CO_2 atmosphere. The H322M cells were cultured with RPMI medium (Thermo Fisher Scientific) containing 10% (v/v) fetal bovine serum (Thermo Fisher Scientific) and penicillin-streptomycin at 37 °C in a humidified 5% CO_2 atmosphere.

After seeding at a density of 1×10^6 cells per 6-well plate, Calu-3 and H322M cells were incubated for 20 h at 37 °C in 5% CO_2. The culture medium was removed and replaced with fresh medium in the presence of (i) 25 μM azithromycin (MCE, Monmouth Junction, NJ, USA), (ii) 50 μM azithromycin, and (iii) 300 μM Zn (Sigma-Aldrich, ST. Louis, MO, USA), (iv) 300 μM Zn and 25 μM azithromycin, (v) 300 μM Zn and 50 μM azithromycin, and incubated for 24 or 48 hours.

RNA isolation

Total RNA was isolated using the PureLink™ RNA mini kit (Thermo Fisher Scientific, Waltham, MA, USA) according to the manufacturer's instructions. The

RNA concentration and quality were assessed using the Quibit 3.0 Fluorometer (Thermo Fisher Scientific). Total RNA samples were stored at −80 °C.

Reverse transcription (RT)

RT reactions were carried out using the superscript III first strand synthesis system (Thermo Fisher Scientific, Waltham, MA, USA). cDNA was synthesized starting from 2 µg of purified total RNA. The reactions in a final volume of 20 µl contained 1x Buffer, DTT, dNTPs, superscript III RT, and 500 ng oligo(dT). Samples were incubated at 65 °C for 5 minutes and 50 °C for 60 minutes, and then the RT enzyme was inactivated by heating to 70 °C for 15 minutes. cDNA samples were stored at -20 °C.

Quantitative PCR (qPCR)

qPCR was carried out with KAPA SYBR®FAST qPCR Master Mix (Wilmington, MA, USA) in a final volume of 20 µl, with 0.3 µM forward and reverse primer and 1 µl of cDNA. Fluorescent detection was performed using the ABI 7500 fast System (Thermo Fisher Scientific) with the following thermal cycling conditions: initial polymerase activation at 95 °C for 3 minutes, followed by 40 cycles of denaturation at 95 °C for 3 seconds and annealing/extension at 60 °C for 30 seconds. After amplification, dissociation (melting) curve analysis was performed to analyze the product melting temperature. Each sample was amplified in triplicate wells. Negative (no template) controls were included in each assay. The results were analyzed using ABI 7500 Fast System Software. The threshold cycle (Ct) at which the amount of amplified target reached a fixed threshold was determined. Relative expression was calculated using the $2^{-\Delta\Delta Cq}$ method. The results were analyzed and are shown as the fold change relative to each control group.

Gene	Primer sequences (5'→3')	Product size (bp)
RPLP0	F: TGGTCATCCAGCAGGTGTTCGA	119

	R: ACAGACACTGGCAACATTGCGG	
GAPDH	F: GAAGGTGAAGGTCGGAGT R: GAAGATGGTGATGGGATTTC	172
ACE2	F: GGACCCAGGAAATGTTCAGA R: GGCTGCAGAAAGTGACATGA	238
IKBα	F: GAAGTGATCCGCCAGGTGAA R: CTGCTCACAGGCAAGGTGTA	189
MUC1	F: CCTACCATCCTATGAGCGAGTAC R: GCTGGGTTTGTGTAAGAGAGGC	136

Table 1. Primers used for aPCR.

Western blot

Cells were scraped with lysis buffer (1% Triton X-100, 20 mM Tris pH 7.4, 150 mM NaCl, and protease inhibitors) on an ice tray, and cell lysates were subjected to western blot analysis. Protein samples were first separated by SDS–PAGE and then transferred to a PVDF membrane. Primary antibodies were applied to detect specific protein expression, followed by incubation with appropriate HRP-conjugated secondary antibodies. Protein signals were developed using an enhanced chemiluminescence reagent (Biomate, Taiwan) and detected by a BIO-RAD ChemiDoc^{TM} MP imaging system (BIO-RAD, Hercules, CA, USA). Western blots were carried out with ACE-2 antibody (Bioss, Woburn, MA, USA), IKB-α antibody (Santa Cruz, Dallas, TX, USA) and PARP antibody (Cell Signaling, Danvers, MA, USA); α-tubulin antibody (Novus, Littleton, CO, USA) was used as a loading control.

Statistical analysis

For statistical analysis, the mean and standard errors were calculated by using GraphPad Prism software version 9 (GraphPad Software Inc., San Diego, CA, USA). Student's t-tests were used to determine significant differences between two experimental conditions. Data were presented as mean + SEM.

Author contributions

YKC, TTH, MCL and BRL conceived and designed the research; CWC and YJH performed the experiments; CWC and YKC wrote the manuscript and generated the illustrations. TTH, YKC, BRL, YPL and CYC reviewed and edited the manuscript; All authors read and approved the final manuscript.

Acknowledgments

We are grateful to Ann-Lii Cheng (Dean of National Taiwan University Cancer Center) and Dr. Ming-Hua Shiao, Dr. Yao-Joe Joseph Yang (Chiefs of Taiwan Instrument Research Institute, National Applied Research Laboratories) for organization and coordination between the groups. We thank staff of the Second Core Lab, Department of Medical Research, National Taiwan University Hospital for technical support during the study. We thank Chao-Chi Ho (National Taiwan University Hospital) for technical support of lung cancer cell lines.

Competing Interests

Disclosures: The authors declare no competing interests exist.

Reference

1. **Aghai ZH, Kode A, Saslow JG, Nakhla T, Farhath S, Stahl GE, Eydelman R, Strande L, Leone P, and Rahman I**. Azithromycin suppresses activation of nuclear factor-kappa B and synthesis of pro-inflammatory cytokines in tracheal aspirate cells from premature infants. *Pediatr Res* 62: 483-488, 2007.
2. **Bao S, Liu MJ, Lee B, Besecker B, Lai JP, Guttridge DC, and Knoell DL**. Zinc modulates the innate immune response in vivo to polymicrobial sepsis through regulation of NF-kappaB. *Am J Physiol Lung Cell Mol Physiol* 298: L744-754, 2010.
3. **Cavalcanti AB, Zampieri FG, Rosa RG, Azevedo LCP, Veiga VC, Avezum A, Damiani LP, Marcadenti A, Kawano-Dourado L, Lisboa T, Junqueira DLM, de Barros ESPGM, Tramujas L, Abreu-Silva EO, Laranjeira LN, Soares AT, Echenique LS, Pereira AJ, Freitas FGR, Gebara OCE, Dantas VCS, Furtado RHM, Milan EP, Golin NA, Cardoso FF, Maia IS, Hoffmann Filho CR, Kormann APM, Amazonas RB, Bocchi de Oliveira MF, Serpa-Neto A, Falavigna M, Lopes RD, Machado FR, Berwanger O, and Coalition Covid-19 Brazil II**. Hydroxychloroquine with or without Azithromycin in Mild-to-Moderate Covid-19. *N Engl J Med* 2020.
4. **Derwand R, Scholz M, and Zelenko V**. COVID-19 outpatients: early risk-stratified treatment with zinc plus low-dose hydroxychloroquine and azithromycin: a retrospective case series study. *Int J Antimicrob Agents* 56: 106214, 2020.
5. **Finzi E**. Treatment of SARS-CoV-2 with high dose oral zinc salts: A report on four patients. *Int J Infect Dis* 99: 307-309, 2020.
6. **Foster KA, Avery ML, Yazdanian M, and Audus KL**. Characterization of the Calu-3 cell line as a tool to screen pulmonary drug delivery. *Int J Pharm* 208: 1-11, 2000.
7. **Furtado RHM, Berwanger O, Fonseca HA, Correa TD, Ferraz LR, Lapa MG, Zampieri FG, Veiga VC, Azevedo LCP, Rosa RG, Lopes RD, Avezum A, Manoel ALO, Piza FMT, Martins PA, Lisboa TC, Pereira AJ, Olivato GB, Dantas VCS, Milan EP, Gebara OCE, Amazonas RB, Oliveira MB, Soares RVP, Moia DDF, Piano LPA, Castilho K, Momesso R, Schettino GPP, Rizzo LV, Neto AS, Machado FR, Cavalcanti AB, and Investigators CC-BI**. Azithromycin in addition to standard of care versus standard of care alone in the treatment of patients admitted to the hospital with severe

COVID-19 in Brazil (COALITION II): a randomised clinical trial. *Lancet* 396: 959-967, 2020.

8. **Gautret P, Lagier JC, Parola P, Hoang VT, Meddeb L, Sevestre J, Mailhe M, Doudier B, Aubry C, Amrane S, Seng P, Hocquart M, Eldin C, Finance J, Vieira VE, Tissot-Dupont HT, Honore S, Stein A, Million M, Colson P, La Scola B, Veit V, Jacquier A, Deharo JC, Drancourt M, Fournier PE, Rolain JM, Brouqui P, and Raoult D**. Clinical and microbiological effect of a combination of hydroxychloroquine and azithromycin in 80 COVID-19 patients with at least a six-day follow up: A pilot observational study. *Travel Med Infect Dis* 34: 101663, 2020.

9. **Gielen V, Johnston SL, and Edwards MR**. Azithromycin induces anti-viral responses in bronchial epithelial cells. *Eur Respir J* 36: 646-654, 2010.

10. **Group RC, Horby P, Mafham M, Linsell L, Bell JL, Staplin N, Emberson JR, Wiselka M, Ustianowski A, Elmahi E, Prudon B, Whitehouse T, Felton T, Williams J, Faccenda J, Underwood J, Baillie JK, Chappell LC, Faust SN, Jaki T, Jeffery K, Lim WS, Montgomery A, Rowan K, Tarning J, Watson JA, White NJ, Juszczak E, Haynes R, and Landray MJ**. Effect of Hydroxychloroquine in Hospitalized Patients with Covid-19. *N Engl J Med* 383: 2030-2040, 2020.

11. **Hirano T, and Murakami M**. COVID-19: A New Virus, but a Familiar Receptor and Cytokine Release Syndrome. *Immunity* 52: 731-733, 2020.

12. **Hoffmann M, Kleine-Weber H, Schroeder S, Kruger N, Herrler T, Erichsen S, Schiergens TS, Herrler G, Wu NH, Nitsche A, Muller MA, Drosten C, and Pohlmann S**. SARS-CoV-2 Cell Entry Depends on ACE2 and TMPRSS2 and Is Blocked by a Clinically Proven Protease Inhibitor. *Cell* 181: 271-280 e278, 2020.

13. **Hou YJ, Chiba S, Halfmann P, Ehre C, Kuroda M, Dinnon KH, 3rd, Leist SR, Schafer A, Nakajima N, Takahashi K, Lee RE, Mascenik TM, Graham R, Edwards CE, Tse LV, Okuda K, Markmann AJ, Bartelt L, de Silva A, Margolis DM, Boucher RC, Randell SH, Suzuki T, Gralinski LE, Kawaoka Y, and Baric RS**. SARS-CoV-2 D614G variant exhibits efficient replication ex vivo and transmission in vivo. *Science* 370: 1464-1468, 2020.

14. **Hou YJ, Okuda K, Edwards CE, Martinez DR, Asakura T, Dinnon KH, 3rd, Kato T, Lee RE, Yount BL, Mascenik TM, Chen G, Olivier KN, Ghio A, Tse LV, Leist SR, Gralinski LE, Schafer A, Dang H, Gilmore R, Nakano S, Sun L, Fulcher ML, Livraghi-Butrico A, Nicely NI, Cameron M, Cameron C, Kelvin DJ, de Silva A, Margolis DM, Markmann A, Bartelt L, Zumwalt R, Martinez FJ, Salvatore SP, Borczuk A, Tata PR, Sontake V, Kimple A, Jaspers I, O'Neal WK, Randell SH, Boucher RC, and Baric RS**. SARS-CoV-2 Reverse Genetics Reveals a Variable Infection Gradient in the Respiratory Tract. *Cell* 182: 429-446 e414, 2020.

15. **Huang J, Hume AJ, Abo KM, Werder RB, Villacorta-Martin C, Alysandratos KD,**

Beermann ML, Simone-Roach C, Lindstrom-Vautrin J, Olejnik J, Suder EL, Bullitt E, Hinds A, Sharma A, Bosmann M, Wang R, Hawkins F, Burks EJ, Saeed M, Wilson AA, Muhlberger E, and Kotton DN. SARS-CoV-2 Infection of Pluripotent Stem Cell-Derived Human Lung Alveolar Type 2 Cells Elicits a Rapid Epithelial-Intrinsic Inflammatory Response. *Cell Stem Cell* 2020.

16. **Inoue D, Furubayashi T, Tanaka A, Sakane T, and Sugano K**. Quantitative estimation of drug permeation through nasal mucosa using in vitro membrane permeability across Calu-3 cell layers for predicting in vivo bioavailability after intranasal administration to rats. *Eur J Pharm Biopharm* 149: 145-153, 2020.

17. **Jothimani D, Kailasam E, Danielraj S, Nallathambi B, Ramachandran H, Sekar P, Manoharan S, Ramani V, Narasimhan G, Kaliamoorthy I, and Rela M**. COVID-19: Poor outcomes in patients with zinc deficiency. *Int J Infect Dis* 100: 343-349, 2020.

18. **Kumar A, Kubota Y, Chernov M, and Kasuya H**. Potential role of zinc supplementation in prophylaxis and treatment of COVID-19. *Med Hypotheses* 144: 109848, 2020.

19. **Kumssa DB, Joy EJ, Ander EL, Watts MJ, Young SD, Walker S, and Broadley MR**. Dietary calcium and zinc deficiency risks are decreasing but remain prevalent. *Sci Rep* 5: 10974, 2015.

20. **Lagier JC, Million M, Gautret P, Colson P, Cortaredona S, Giraud-Gatineau A, Honore S, Gaubert JY, Fournier PE, Tissot-Dupont H, Chabriere E, Stein A, Deharo JC, Fenollar F, Rolain JM, Obadia Y, Jacquier A, La Scola B, Brouqui P, Drancourt M, Parola P, Raoult D, and force IC-T**. Outcomes of 3,737 COVID-19 patients treated with hydroxychloroquine/azithromycin and other regimens in Marseille, France: A retrospective analysis. *Travel Med Infect Dis* 101791, 2020.

21. **Li G, He X, Zhang L, Ran Q, Wang J, Xiong A, Wu D, Chen F, Sun J, and Chang C**. Assessing ACE2 expression patterns in lung tissues in the pathogenesis of COVID-19. *J Autoimmun* 112: 102463, 2020.

22. **Liao M, Liu Y, Yuan J, Wen Y, Xu G, Zhao J, Cheng L, Li J, Wang X, Wang F, Liu L, Amit I, Zhang S, and Zhang Z**. Single-cell landscape of bronchoalveolar immune cells in patients with COVID-19. *Nat Med* 26: 842-844, 2020.

23. **Lu W, Liu X, Wang T, Liu F, Zhu A, Lin Y, Luo J, Ye F, He J, Zhao J, Li Y, and Zhong N**. Elevated MUC1 and MUC5AC mucin protein levels in airway mucus of critical ill COVID-19 patients. *J Med Virol* 2020.

24. **Mathes E, O'Dea EL, Hoffmann A, and Ghosh G**. NF-kappaB dictates the degradation pathway of IkappaBalpha. *EMBO J* 27: 1357-1367, 2008.

25. **McAuley JL, Corcilius L, Tan HX, Payne RJ, McGuckin MA, and Brown LE**. The cell surface mucin MUC1 limits the severity of influenza A virus infection. *Mucosal Immunol* 10: 1581-1593, 2017.

26. **Menzel M, Akbarshahi H, Bjermer L, and Uller L**. Azithromycin induces anti-viral effects in cultured bronchial epithelial cells from COPD patients. *Sci Rep* 6: 28698, 2016.
27. **Onofrio L, Caraglia M, Facchini G, Margherita V, Placido S, and Buonerba C**. Toll-like receptors and COVID-19: a two-faced story with an exciting ending. *Future Sci OA* 6: FSO605, 2020.
28. **Patra R, Chandra Das N, and Mukherjee S**. Targeting human TLRs to combat COVID-19: A solution? *J Med Virol* 2020.
29. **Pelaseyed T, Bergstrom JH, Gustafsson JK, Ermund A, Birchenough GM, Schutte A, van der Post S, Svensson F, Rodriguez-Pineiro AM, Nystrom EE, Wising C, Johansson ME, and Hansson GC**. The mucus and mucins of the goblet cells and enterocytes provide the first defense line of the gastrointestinal tract and interact with the immune system. *Immunol Rev* 260: 8-20, 2014.
30. **Perera M, El Khoury J, Chinni V, Bolton D, Qu L, Johnson P, Trubiano J, McDonald CF, Jones D, Bellomo R, Patel O, and Ischia J**. Randomised controlled trial for high-dose intravenous zinc as adjunctive therapy in SARS-CoV-2 (COVID-19) positive critically ill patients: trial protocol. *BMJ Open* 10: e040580, 2020.
31. **Poulas K, Farsalinos K, and Zanidis C**. Activation of TLR7 and Innate Immunity as an Efficient Method Against COVID-19 Pandemic: Imiquimod as a Potential Therapy. *Front Immunol* 11: 1373, 2020.
32. **Rosenberg ES, Dufort EM, Udo T, Wilberschied LA, Kumar J, Tesoriero J, Weinberg P, Kirkwood J, Muse A, DeHovitz J, Blog DS, Hutton B, Holtgrave DR, and Zucker HA**. Association of Treatment With Hydroxychloroquine or Azithromycin With In-Hospital Mortality in Patients With COVID-19 in New York State. *JAMA* 2020.
33. **Sahebnasagh A, Saghafi F, Avan R, Khoshi A, Khataminia M, Safdari M, Habtemariam S, Ghaleno HR, and Nabavi SM**. The prophylaxis and treatment potential of supplements for COVID-19. *Eur J Pharmacol* 887: 173530, 2020.
34. **Schogler A, Kopf BS, Edwards MR, Johnston SL, Casaulta C, Kieninger E, Jung A, Moeller A, Geiser T, Regamey N, and Alves MP**. Novel antiviral properties of azithromycin in cystic fibrosis airway epithelial cells. *Eur Respir J* 45: 428-439, 2015.
35. **Self WH, Semler MW, Leither LM, Casey JD, Angus DC, Brower RG, Chang SY, Collins SP, Eppensteiner JC, Filbin MR, Files DC, Gibbs KW, Ginde AA, Gong MN, Harrell FE, Jr., Hayden DL, Hough CL, Johnson NJ, Khan A, Lindsell CJ, Matthay MA, Moss M, Park PK, Rice TW, Robinson BRH, Schoenfeld DA, Shapiro NI, Steingrub JS, Ulysse CA, Weissman A, Yealy DM, Thompson BT, Brown SM, National Heart L, and Blood Institute PCTN**. Effect of Hydroxychloroquine on Clinical Status at 14 Days in Hospitalized Patients With COVID-19: A Randomized Clinical Trial. *JAMA* 324: 2165-2176, 2020.

36. **Sibinovska N, Zakelj S, Roskar R, and Kristan K**. Suitability and functional characterization of two Calu-3 cell models for prediction of drug permeability across the airway epithelial barrier. *Int J Pharm* 585: 119484, 2020.
37. **Smith JC, Sausville EL, Girish V, Yuan ML, Vasudevan A, John KM, and Sheltzer JM**. Cigarette Smoke Exposure and Inflammatory Signaling Increase the Expression of the SARS-CoV-2 Receptor ACE2 in the Respiratory Tract. *Dev Cell* 53: 514-529 e513, 2020.
38. **Stellari FF, Sala A, Donofrio G, Ruscitti F, Caruso P, Topini TM, Francis KP, Li X, Carnini C, Civelli M, and Villetti G**. Azithromycin inhibits nuclear factor-kappaB activation during lung inflammation: an in vivo imaging study. *Pharmacol Res Perspect* 2: e00058, 2014.
39. **Tenson T, Lovmar M, and Ehrenberg M**. The mechanism of action of macrolides, lincosamides and streptogramin B reveals the nascent peptide exit path in the ribosome. *J Mol Biol* 330: 1005-1014, 2003.
40. **Tran DH, Sugamata R, Hirose T, Suzuki S, Noguchi Y, Sugawara A, Ito F, Yamamoto T, Kawachi S, Akagawa KS, Omura S, Sunazuka T, Ito N, Mimaki M, and Suzuki K**. Azithromycin, a 15-membered macrolide antibiotic, inhibits influenza A(H1N1)pdm09 virus infection by interfering with virus internalization process. *J Antibiot (Tokyo)* 72: 759-768, 2019.
41. **Ueno K, Koga T, Kato K, Golenbock DT, Gendler SJ, Kai H, and Kim KC**. MUC1 mucin is a negative regulator of toll-like receptor signaling. *Am J Respir Cell Mol Biol* 38: 263-268, 2008.
42. **Walls AC, Park YJ, Tortorici MA, Wall A, McGuire AT, and Veesler D**. Structure, Function, and Antigenicity of the SARS-CoV-2 Spike Glycoprotein. *Cell* 181: 281-292 e286, 2020.
43. **Wessels I, Rolles B, and Rink L**. The Potential Impact of Zinc Supplementation on COVID-19 Pathogenesis. *Front Immunol* 11: 1712, 2020.
44. **Xu G, Qi F, Li H, Yang Q, Wang H, Wang X, Liu X, Zhao J, Liao X, Liu Y, Liu L, Zhang S, and Zhang Z**. The differential immune responses to COVID-19 in peripheral and lung revealed by single-cell RNA sequencing. *Cell Discov* 6: 73, 2020.
45. **Zhou P, Yang XL, Wang XG, Hu B, Zhang L, Zhang W, Si HR, Zhu Y, Li B, Huang CL, Chen HD, Chen J, Luo Y, Guo H, Jiang RD, Liu MQ, Chen Y, Shen XR, Wang X, Zheng XS, Zhao K, Chen QJ, Deng F, Liu LL, Yan B, Zhan FX, Wang YY, Xiao GF, and Shi ZL**. A pneumonia outbreak associated with a new coronavirus of probable bat origin. *Nature* 579: 270-273, 2020.

Figure Legends

Figure 1 Azithromycin (AZT) but not ZnSO4 (Zn) treatment alone decreased endogenous ACE2 expression in the human lower airway H322M cells. (A) Endogenous ACE2 expression was screened by Western blot using beta-actin as a loading control. ACE2-expressing Calu-3 and H322M cell lines were selected for subsequent exploration. (B) H322M cells were treated with serial concentrations of Zn (0, 18.75, 37.5, 75, 150 and 300 μM) for 24 hours, and total RNA was collected for *ACE2* quantitation by real-time qRT-PCR assays. The data were normalized to *GAPDH* expression and presented as the mean ± SEM (n = 3). *ACE2* expression was potentially decreased under 24-hour treatment with 300 μM Zn. This concentration was determined for combination treatment with AZT. (C) H322M cells were treated with a concentration series of AZT (0, 3.125, 3.25, 12.5, 25 and 50 μM) for 24 hours, and total RNA was collected for *ACE2* quantitation by real-time qRT-PCR assays. The data were normalized to *GAPDH* expression and presented as the mean ± SEM (n = 3). (**p = 0.001 to 0.01). *ACE2* expression was significantly decreased under 24-hour treatment with 50 μM AZT. This concentration was adopted for combination treatment with Zn.

Figure 2 Endogenous ACE2 expression in H322M and Calu-3 cells was markedly suppressed by Zn and in combination with AZT in a time- and dose-dependent

manner. (A and B) H322M cells were treated with 25, 50 μM AZT and 300 μM Zn in combination for 24 (A) and 48 (B) hours. Treated cells were lysed for Western blot analysis of ACE2 and PARP with α-actin as a loading control. ACE2 expression was suppressed without detectable cleaved PARP by Zn alone and synergistically with AZT in a time- and dose-dependent manner. IKB-α expression was obviously increased following 24 hours of treatment with 300 μM Zn combined with 50 μM AZT. (C and D) Calu-3 cells were treated with 25, 50 μM AZT and 300 μM Zn in combination for 24 (C) and 48 (D) hours. Compared to H322M treated in the same ways, ACE2 expression was suppressed without detectable cleaved PARP by Zn alone and synergistically with AZT in a more time-dependent manner. Similarly, IKB-α expression was obviously increased following 24 hours of treatment with 300 μM Zn combined with 50 μM AZT.

Figure 3 Endogenous ACE2 and IKBα expression was synergistically regulated by combined treatments of Zn and AZT. (A and B) H322M cells were treated with 25, 50 μM AZT and 300 μM Zn in combination for 24 hours. Total RNA was collected for *ACE2* (A) and *IKBα* (B) quantitation by real-time qRT-PCR assays. The data were normalized to GAPDH expression and presented as the mean ± SEM (n = 3). (*p = 0.01 to 0.05, ** p = 0.001 to 0.01, ***p = 0.0001 to 0.001 and ****p = < 0.0001). Compared to the control and AZT alone, 300 μM Zn synergistically decreased *ACE2* and *IKBα* expression with 25 and 50 μM AZT treatments, respectively. (C and D) Calu-3 cells were treated with 25, 50 μM AZT and 300 μM Zn in combination for 24 hours. Total RNA was collected for *ACE2* (A) and *IKBα* (B) quantitation by real-time qRT-PCR assays. The data were normalized to GAPDH/RPLP0 expression for H322M/Calu-3 cells respectively and presented as the

mean ± SEM (n = 3). (*p = 0.01 to 0.05, ** p = 0.001 to 0.01, ***p = 0.0001 to 0.001 and ****p = < 0.0001). Zn showed a similar synergistic suppressive effect on *ACE2* expression in AZT treated Calu-3 cells. Conversely, *IKBα* expression was synergistically upregulated following 25 and 50 µM AZT treatments combined with 300 µM Zn compared to AZT alone.

Figure 4 Endogenous MUC1 expression was significantly increased by Zn treatment alone and to a lesser degree in combination with AZT. H322M (A) and Calu-3 (B) cells were treated with 25, 50 µM AZT and 300 µM Zn in combination for 24 hours. Total RNA was collected for *MUC1* quantitation by real-time qRT-PCR assays. The data were normalized to GAPDH/RPLP0 expression for H322M/Calu-3 cells respectively and are presented as the mean ± SEM (n = 3). (*p = 0.01 to 0.05, ** p = 0.001 to 0.01, ***p = 0.0001 to 0.001 and ****p = < 0.0001). Compared to the control, *MUC1* expression was significantly increased following 300 µM Zn treatment alone and to a lesser degree combined with AZT in H322M and Calu-3 cells. In H322M, *MUC1* expression was synergistically increased following 50 µM AZT treatments combined with 300 µM Zn compared to AZT alone. In Calu-3 cells, *MUC1* expression was synergistically increased following 25 and 50 µM AZT treatments combined with 300 µM Zn compared to AZT alone.

A. Baseline ACE2 expression

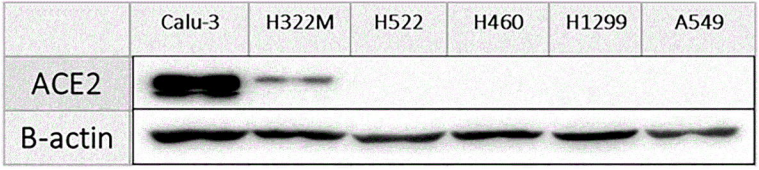

B. Zn Dosing, H322M

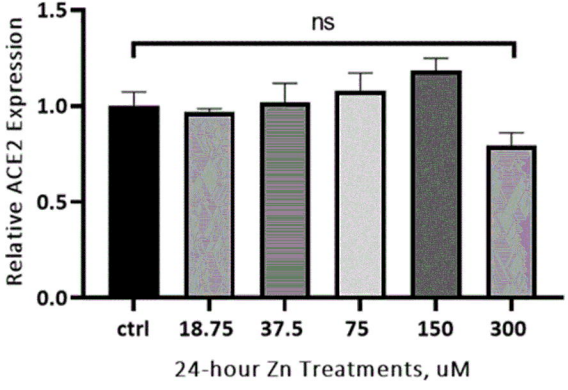

C. AZT Dosing, H322M

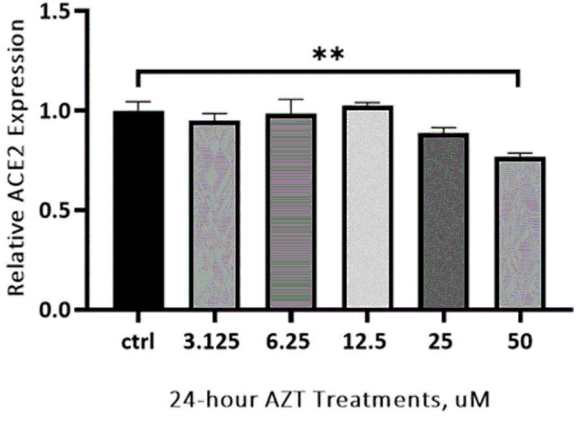

A. H322M, 24-hour Treatments

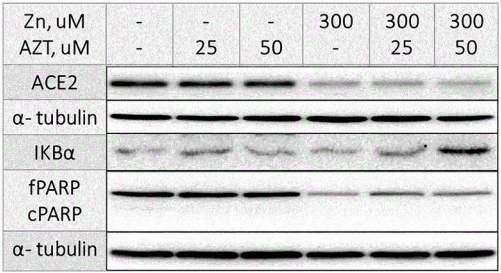

B. H322M, 48-hour Treatment

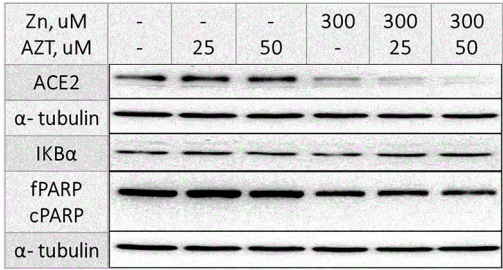

C. Calu-3, 24-hour Treatment

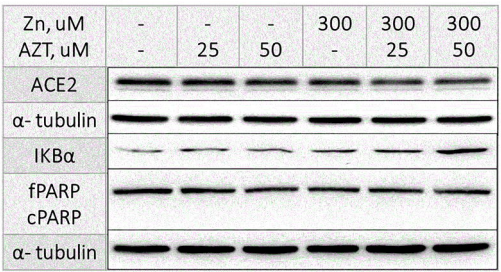

D. Calu-3, 48-hour Treatment

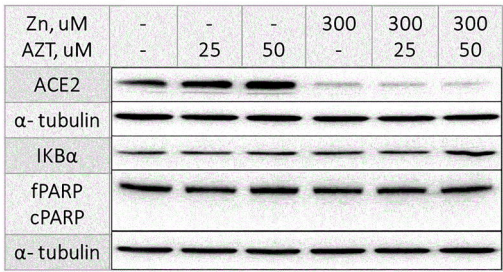

A. ACE2 expression, H322M

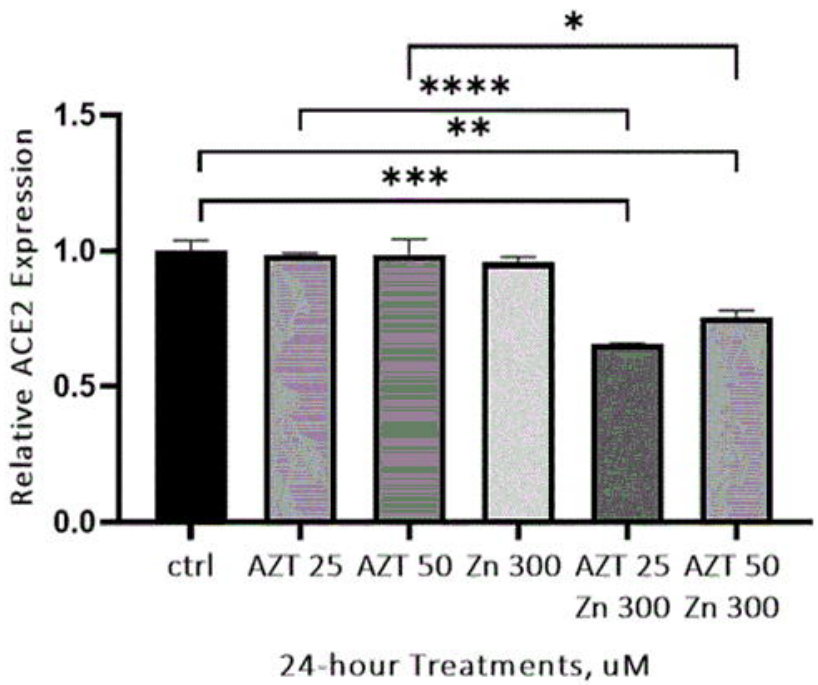

B. IKBalpha expression, H322M

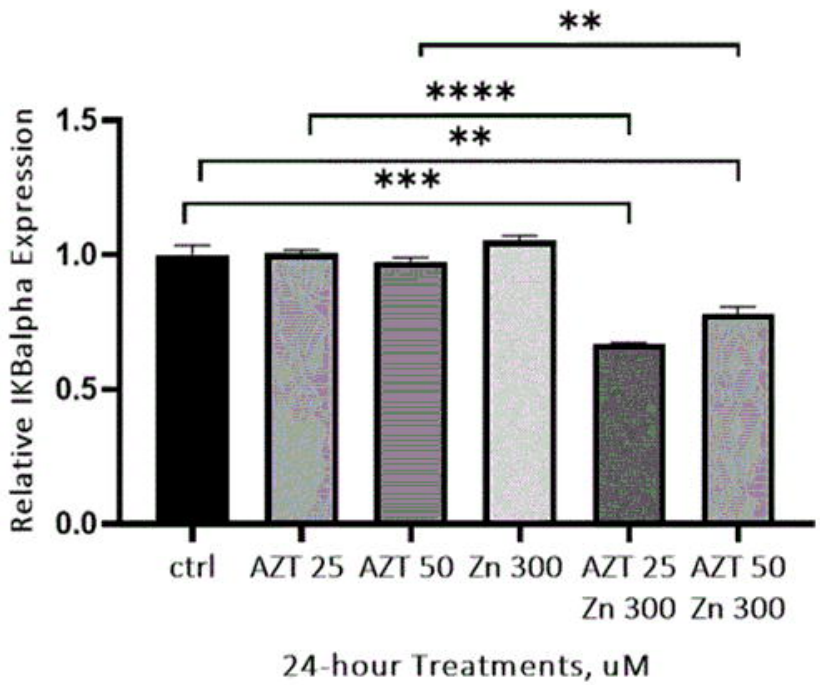

C. ACE2 expression, Calu-3

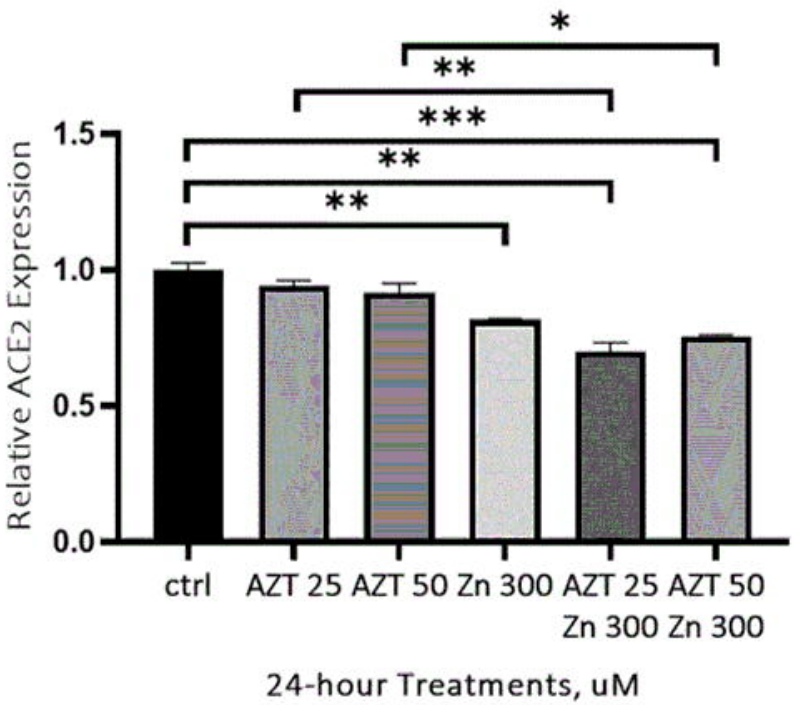

D. IKBalpha expression, Calu-3

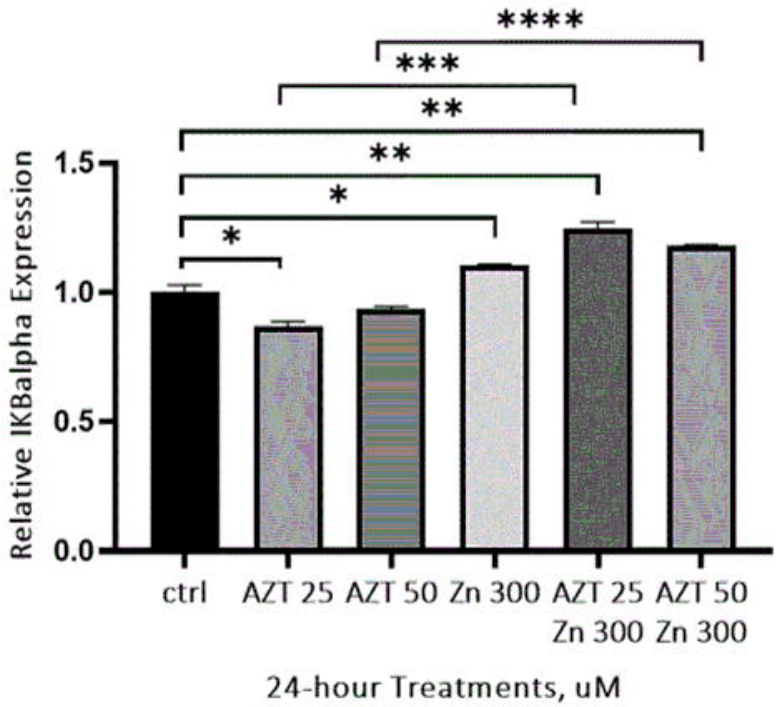

A. H322M

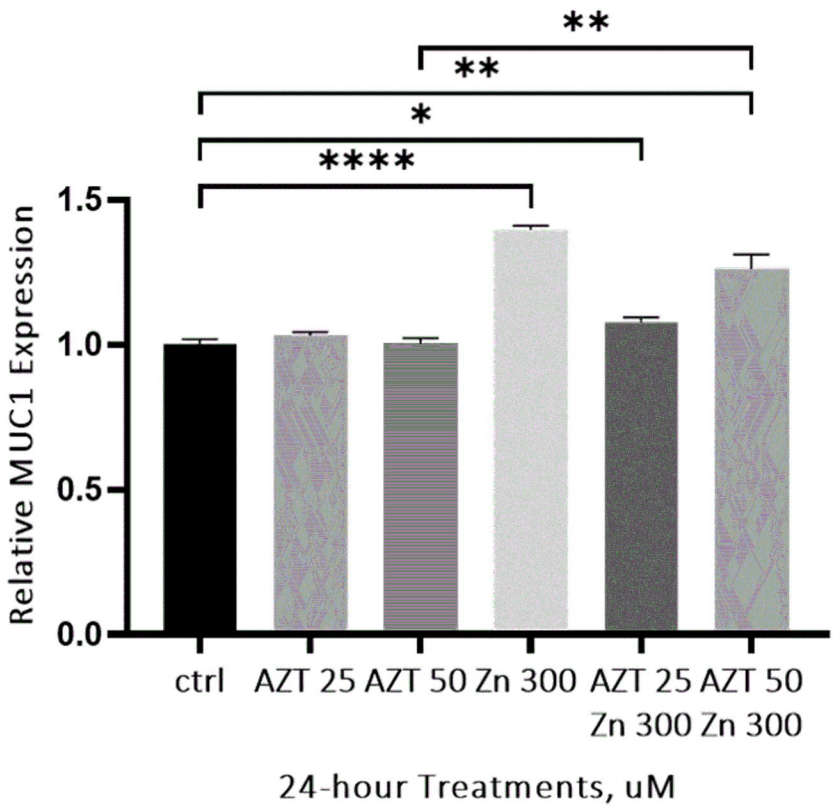
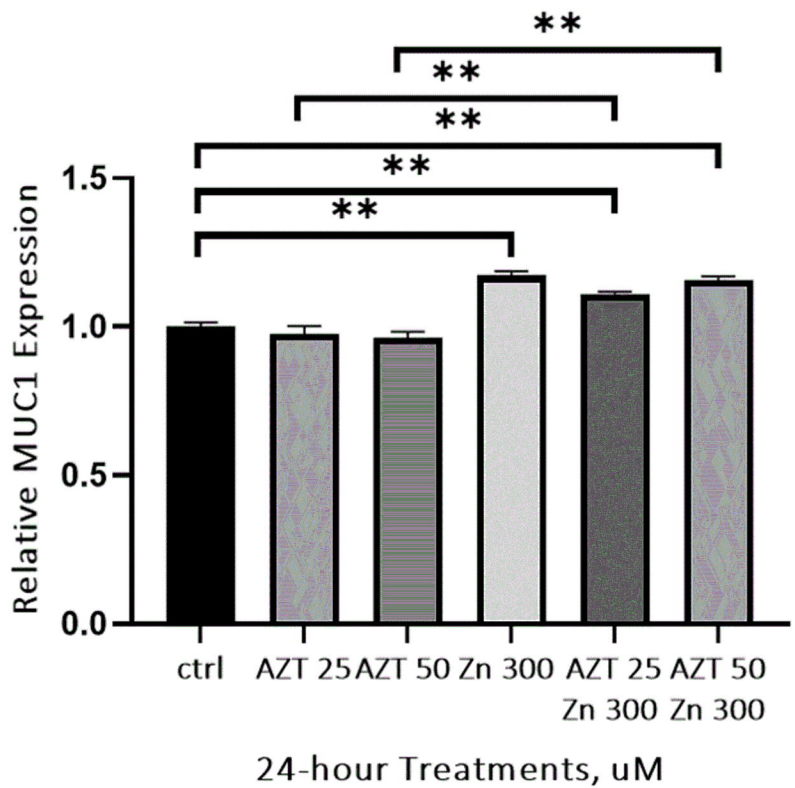
B. Calu-3